

R. Abächerli
C. Pasquier
F. Odille
M. Kraemer
J.-J. Schmid
J. Felblinger

Suppression of MR gradient artefacts on electrophysiological signals based on an adaptive real-time filter with LMS coefficient updates

Received: 27 May 2004
Accepted: 19 April 2004
Published online: 7 February 2005
© ESMRMB 2005

R. Abächerli (✉) · C. Pasquier · F. Odille
J. Felblinger
Interventional and Diagnostic Adaptive
Imaging (IADI)
Tour Drouet
CHU Nancy Brabois
Rue de Morvan
54511 Vandoeuvre-les-Nancy, France
E-mail: roger.abaecherli@schiller.ch
Tel.: +41-41-7664341
Fax: +41-41-7610880

R. Abächerli · M. Kraemer · J.-J. Schmid
SCHILLER, Wissembourg, France and
Baar, Switzerland

Abstract Electrocardiogram (ECG) acquisition is still a challenge as gradient artefacts superimposed on the electrophysiological signal can only be partially removed. The signal shape of these artefacts can be similar to the QRS-complex, causing possible misinterpretation during patient monitoring and false triggering/gating of the MRI. For their real-time suppression, an adaptive filter is proposed. The adaptive filter is based on the noise-canceller configuration with LMS coefficient updates. The references of the noise canceller are the three gradient signals that are acquired simultaneously with the noisy ECG. Tests were done on patients, on volunteers and using an MR-safe ECG simulator. The noise canceller's performance was measured offline, simulating real-time processing by point-by-point operations. To create worst-case scenarios, clinical

sequences with strong- and fast-switching gradients have been chosen. The noise-cancelling filter reduces the gradient artefacts' peak amplitudes by 80–99% after adaptation, without changing the desired ECG signal shape. The estimated reduction of total average power of the MR gradient artefacts is 62–98%. The proposed filter is capable of reducing artefacts due to strong- and fast-switching gradients in real-time applications and worst-case situations. The quality of the ECG is sufficiently high that a standard one-lead QRS-detector can be used for gating/triggering the MRI. For permanent patient monitoring, further improvements are needed.

Keywords ECG · Gradient artefacts · Magnetic resonance imaging · MRI triggering/gating · Physiologic monitoring

Introduction

The acquisition of electrophysiological signals (such as ECG or EEG) at diagnostic signal quality during MRI has become the focus of a number of research laboratories, with the aim of finding a correlation between the physiological signal and the MR image. The EEG can be correlated with the fMRI, while the ECG or SpO₂ is needed for gating/triggering the MRI, especially for cardiac MRI. Imaging a moving organ such as the heart requires about 10–15 heart cycles, for which each MR sequence must be

triggered exactly at the same location within the cardiac cycle. Peripheral pulseoxymetry (SpO₂) is sometimes considered a more robust method than the electrocardiogram (ECG). Its acquisition and transmission is purely optical so that no interference with the MR equipment occurs, minimizing the risk of burns for the patient. However, ECG is preferred as the electrical activity of the heart bears a constant relationship to its mechanical activity, and also in cases where patient monitoring is required. Furthermore, the R-wave, the most easily recognized feature, precedes the mechanical systole. Unfortunately, the

ECG suffers from interference with the MR scanner causing possible misinterpretation during patient monitoring and false triggering/gating of the MRI. To overcome the problem of such interference when triggering/gating the MRI, a solution based on the vector cardiogram [1] and another solution based on the MR image [2] have been proposed. Unfortunately, these solutions are not applicable to patient monitoring.

The main interferences overlying the desired electrophysiological signal are the following: (1) Artefacts due to magnetic induction. It can easily be seen that whenever the magnetic flux changes, a voltage is induced. The change of magnetic flux can either be caused by a movement of the lead wires or electrodes due to patient movement, or by a change of the local magnetic field due to switching MR gradients. (2) Voltages induced by the blood flow [3] (the Hall effect is often referred to as a magnetohydrodynamic effect in the case of the ECG, and as a cardioballogram in the case of the EEG). (3) Artefacts due to radio-frequency (RF) induction that the MR scanner emits at the corresponding Larmor frequency.

The frequency of the RF induction exceeds the maximum frequency of the desired physiological signal by factors. The RF induction problem is usually solved by shielding the ECG sensor and using adequate HF filters. Artefacts due to patient movement can be partially prevented by asking the patient for cooperation or fixing the patient's position. Median templates are calculated for partial suppression of the artefacts due to Hall effect [4]. Gradient artefacts (due to the switching MR gradient field) can be partially reduced by minimizing the size of the ECG acquisition system and using optical transmission instead of long lead wires [5].

In a recent paper, Lui et al. [6] have theoretically shown that the time-varying magnetic field affects the cardiac electric activity, increasing the risk of cardiac arrhythmia in patients with cardiac disease. To analyse this influence (i.e. possible heart arrhythmia) and to ensure accurate monitoring of such patients, an ECG of sufficient quality is needed. Several methods for reducing signal artefacts superimposed on the biomedical signal have been proposed. Most of them concentrate on the EEG for fMRI applications and often use a predefined MR image sequence [4, 7–9]. Offline suppression of signal artefacts due to MR gradients on ECG has already been proposed in [10], although this is not applicable to the real-time case, and in [11], for which unfortunately no performance results are given.

In summary, we are looking for a real-time filter with the following goals. Firstly, accurate and constant delayed online detection of the R-wave should be possible in order to get cardiac MR images of sufficient quality [12]. Secondly, the person supervising the patient lying in the MRI tunnel can only interpret the physiological signal accurately when the signal quality prevents false interpretation

of physiological heart activity. And thirdly, the real-time filter should work for any clinically relevant MR sequence.

Methods

The real-time suppression of gradient artefacts is based on the noise-canceller configuration for adaptive filters [15,16]. This configuration needs a primary input including the desired signal and additive noise. The noise must be correlated with the reference input. In our case (Fig. 1), we use three different filters (each calculates on one spacial axis). Therefore, three reference signals G_x , G_y and G_z are acquired from the gradient amplifier of the MR scanner. The gradient-disturbed ECG is acquired as the primary input with an optical sensor, with short high-resistive carbon wires lying near the patient. This minimizes the risk of burns due to RF interference during ECG acquisition [13, 14].

The tests were performed on a 1.5-T MRI (GE Signa with Excite II, Milwaukee, MI, USA). The ECG was acquired using the optical ECG sensor of the patient-monitoring system Maglife (SCHILLER Médical, France). Gradients and ECG were acquired simultaneously on a PC with 10-kHz sampling frequency. In order to get a large range for the estimated total average power of the MR gradient artefacts, clinical sequences were chosen by varying their parameters and placing the electrodes on different locations on the chest. To create worst-case scenarios, sequences with strong- and fast-switching magnetic gradients (diffusion with FOV smaller than 10 cm, black-blood sequences, head images etc.) were also chosen. The ECG was acquired from five volunteers working at our laboratory (aged from 21 to 42, weight from 65 kg to 83 kg), seven patients or using an MR-safe ECG simulator. The ECG simulator was designed to obtain more comparable and objective ECG recordings.

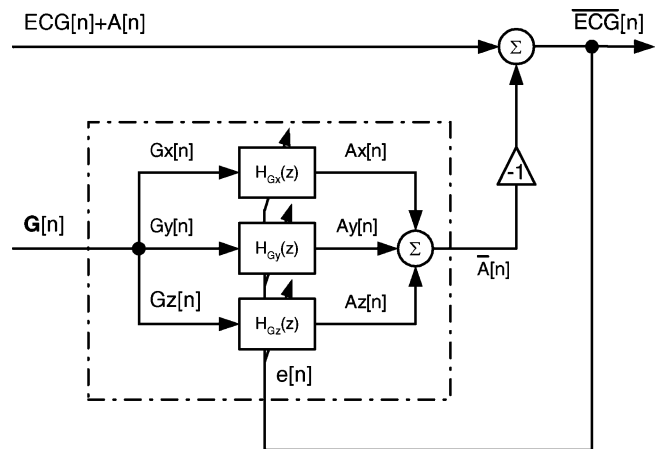


Fig. 1 The gradient artefact overlying the desired ECG is suppressed by the noise-canceller filter with LMS coefficient updates using three reference signals (G_x , G_y and G_z). The MR gradient artefact $A[n]$ (which is the sum of three artefacts $A_x[n]$, $A_y[n]$, $A_z[n]$) is assumed to be additive noise and to be correlated with the reference signals

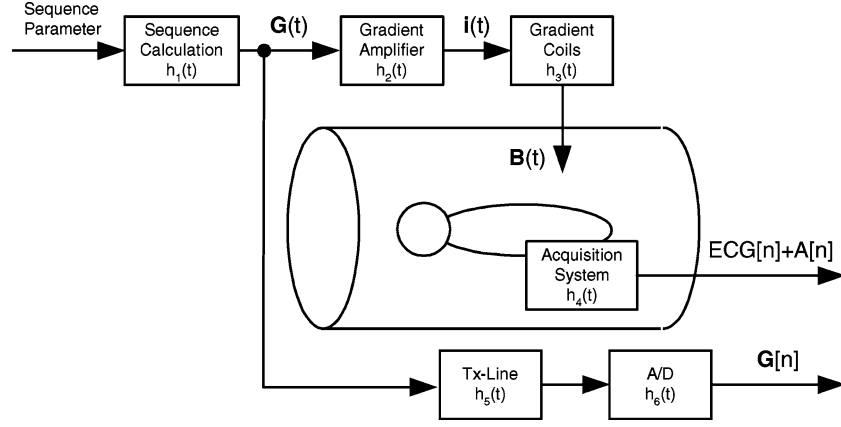


Fig. 2 Simplified model of the gradient artefact generation and our acquisition system. Each part of the acquisition system is modelled by a subtask in order to describe its physical behaviour. The unknown total transfer function of the acquired gradient signals $G[n] = (G_x[n], G_y[n], G_z[n])^T$ to the gradient artefact $A[n]$ must be found by the adaptive noise canceller

Our home-made MR-safe ECG simulator consists of a signal generator protected by a double copper Faraday cage simulating a heart rate from 60 to 90 beats per minute.

Physical behaviour

In order to choose an adequate adaptive filter and interpret its performance, we need to analyse the acquisition system (Fig. 2). We assumed that the noise and signal artefacts which overlie the desired ECG are additive. From the sequence parameters (TE, TR, FOV, image matrix, orientation of slices, number of slices and so on), which are entered into the MR station, the sequence calculator unit calculates the gradient curves $G(t) = [G_x(t), G_y(t), G_z(t)]^T$ for the x , y and z axes in the MR bore. These gradient signals are used by the gradient amplifier, which powers the gradient coils. The changing magnetic field in the MR tunnel provokes the gradient artefacts overlying the ECG signal. Many different sequences and sequence parameters exist. For simplification, the gradient signals can be interpreted as a set of stochastic signals (the output of a system with stochastic input). The sequence calculation unit, modelled by $h_1(t)$, is a time-invariant and deterministic system as long as the sequence is not changed or sequence parameters are not modified (which is not the case during one MRI session). The gradient amplifier and the gradient coils are always time-invariant and deterministic systems. Therefore, they can be modelled by time-invariant system blocks with corresponding transfer functions $h_2(t)$ and $h_3(t)$. The transfer function $h_1(t)$ is not of primary interest in our design. The transfer function $h_2(t)$ corresponds to the conversion of the gradient signal into gradient coil

currents. The transfer function $h_3(t)$ is based on the physical law of Biot–Savart. However, the design of the gradient coils for perfect linear magnetic gradients in the MR bore is much more complicated and not known in full detail. The transfer function $h_4(t)$, which is the induction of the magnetic gradients into the human tissue, the ECG sensor and the lead wires provoking the gradient artefacts in the ECG signal, is very difficult to model and has not yet been calculated. The coaxial cables between the gradient signal outputs of the gradient amplifier and the acquisition PC can be described by a transmission line that is modelled by $h_5(t)$. The AD conversion is summarized by the transfer function $h_6(t)$.

The designed, adaptive filter simulates the convolution of $h_2(t)$ to $h_4(t)$. Simplifying the overall transfer function as much as possible to get a global idea of the physical effects inside the MR bore yields:

$$A[n] = f(\vec{B}(t)) \approx -\frac{d\phi}{dt} = -\frac{d(\vec{B} \cdot \vec{A})}{dt} = -\frac{d((\vec{G}(t) \cdot \vec{r}(t)) \cdot A(t))}{dt}.$$

where $A[n]$ is the discrete acquired signal of the gradient artefact due to the changing magnet gradient, $B(t)$ is the magnetic field in the MR tunnel, $G(t)$ is the vector containing the three gradient signals G_x , G_y , and G_z , $r(t)$ are the coordinates x , y and z in the MR tunnel where induction occurs and $A(t)$ is the active area where the magnetic flux flows through the human tissue, the lead wires and the ECG sensor. Furthermore, the adaptive filter needs to perform the inversion of $h_5(t)$ and $h_6(t)$ because the discrete version of the acquired gradient signal is fed into the adaptive noise canceller. Thus, the adaptive filter must calculate the three transfer functions in order to estimate the MR gradient artefacts for each axis (x , y and z) as follows:

$$\bar{A}_i[n] = h_{G_i}[n] * G_i[n], \quad i = x, y, z.$$

Where the transfer function for each direction is defined as:

$$h_{G_i}[n] = h_{4_i}[n] * h_{3_i}[n] * h_{2_i}[n] * h_{5_i}^{-1}[n] * h_{6_i}^{-1}[n] * G_i[n], \quad i = x, y, z.$$

The three transfer functions h_{G_x} , h_{G_y} and h_{G_z} are unknown and must be found by the three filter parts of our noise canceller. If all transfer functions remain unchanged, a discrete linear time-invariant system with fixed impulse responses could be used instead of the adaptive filter [9]. In this case, each impulse response must be found based on the corresponding gradient signal where the other two gradient signals need to be zero. Every time the sequence is changed, a new set of impulse responses is required. Furthermore, as soon as the electrodes, the lead wire or the ECG sensor moves in the MR tunnel or the magnetic behaviour of the human tissue changes, the transfer functions can become time-variant. As the patient breathes, at least the electrodes and the connected lead wires will move and force a change in the induction of the switching magnetic gradients (change of vector r and magnetic active area $A(t)$). Thus an adaptive filter, which continuously follows such changes, would be a more adequate solution.

Adaptive noise cancelling

We have seen that the overall transfer function is based on nonlinear physical effects. We used a linear time-varying finite impulse response (FIR) kernel to verify that it is possible to track the nonlinear physical effects:

$$A_i[n] = \sum_{k=0}^{N-1} w_i[k] \cdot G_i[n-k], \quad i = x, y, z$$

where N ($=256/1$ kHz) is the filter window length and $w_i[k]$ are the changing filter coefficients. Our goal was to use a simple adaptive filter that does not need any type of higher-order calculation or include matrix calculations. We therefore used the least-mean-square (LMS) algorithm proposed by Widrow et al. [16] to update the filter coefficients by replacing the error signal $\varepsilon[n]$ with the corrected ECG (i.e. the output of the noise canceller):

$$w_i[n+1] = w_i[n] + 2\mu \cdot \varepsilon[n] \cdot G_i[n], \quad i = x, y, z$$

The step size μ , which controls the convergence rate, was set to $0.15/(\text{window filter length times variance of reference signal})$. The transfer functions are learned by the filter coefficients during the MR parameter optimization phase (prescan) and applied when the image sequence starts. During the image sequence, the noise canceller continues to adapt, following the changes in the MR bore. The noise canceller's performance was measured using Matlab (Mathworks – MA) simulating real-time processing

by point-by-point operations. Two variants for the reference signals $G = [G_x, G_y, G_z]^T$ have been tested: (1) they have been resampled to 500 Hz including anti-aliasing filtering without any further preprocessing. (2) They have been resampled to 500 Hz including anti-aliasing filtering, whereby the DC values of the three gradient buffers $G_i[0, N-1]$ were subtracted.

Tests and evaluation of filter efficiency

In noise suppression cases where the performance of a filter is measured, the signal-to-noise ratio (SNR), defined as the ratio between the total average power of the desired signal and the total average power of the noise, is used:

$$\text{SNR} = \frac{E[s^2(n)]}{E[n^2(n)]} = \frac{E[(\text{ECG}(n))^2]}{E[A^2(n)]}.$$

In other cases, the mean square error (MSE) defined as the expected value of the squared difference between the desired signal and its estimate, can also be used:

$$\text{MSE} = E[(s(n) - \hat{s}(n))^2].$$

In our case, we want to change the ECG signal as little as possible meaning that the total average power of the ECG, $E[(\text{ECG}(n))^2]$, remains as constant as possible. Taking the SNR as a measurement of the performance of our filter therefore does not make much sense, as the total average power of the ECG can vary considerably between different subjects. In such cases, the SNR is improved even if the total average power of the noise remains constant. A intra-subject comparison between different cases would therefore be possible, but not an inter-subject comparison. Tracking the total average power of the noise is preferable. Unfortunately, this value can only be estimated.

Using the ECG simulator, the total average power of the noise can be estimated by deducting the ECG from the acquired signal as the ECG curve does not change and is already known. The total average power of the noise can thereby be accurately calculated. For volunteers or patients, the average of the ECG beats of a subject can be estimated and then deducted from the acquired signal. In this case, two error sources can be identified. Firstly, the uncorrelated noise is filtered out of the average ECG beat, but correlated noise (as the MR gradient artefact can be when the ECG is used for triggering/gating) will remain. Secondly, the average ECG beat does not include changes in the ECG (amplitude modulation due to respiration, heart rate changes, arrhythmias and similar effects). To summarize, the estimated noise signal does not always contain all noise components and could contain signal parts of the ECG. For the correct calculation of the mean square error (MSE), the artefact-free signal and the filtered signal must be known. Another performance

measurement may be to calculate of the reduction of the MR gradient artefacts' peak amplitudes. For each signal the peaks of the MR gradient artefacts are identified and their amplitudes measured. The results before and after filtering are compared.

We propose five different test methods to evaluate the performance of the adaptive filter.

- 1) Calculating the MSE between the ECG signals before and after filtering for zero gradient signals (i.e. no MR imaging and no MR gradient artefacts). This test is needed to show that the filter does not change the ECG when no MR image is taken.
- 2) Calculating the MSE between the ECG signal before and after filtering if no (or very small) artefacts could be found on the acquired signal. This test will show by how much the adaptive filter suppresses ECG signal parts which could be correlated with the MR gradient signals.
- 3) Calculating the reduction of the estimated signal power and amplitude peaks of the MR gradient artefacts before and after filtering using the home-made ECG simulator. This test directly measures the efficiency of MR gradient artefact suppression but will not include MR gradient artefacts induced in human tissue.
- 4) Calculating the reduction of total average power and peak amplitudes in the acquired signals which only include MR gradient artefacts (ECG is measured on leg or arm, where no or very small parts of the ECG signal are present).
- 5) Calculating the reduction of the estimated signal power of the complete acquired signal, and comparing the peak amplitudes of the MR gradient artefacts before and after filtering on ECG signals recorded on volunteers and patients.

Results

In tests 1 and 2 (zero MR gradient signals and no MR gradient artefacts), the adaptive noise canceller filter does not change the ECG, as the largest value of MSE remains minimal ($8.0 \times 10^{-4} \mu\text{V}^2$ in the case of zero gradient signals and $6.2 \times 10^{-2} \mu\text{V}^2$ in the case of zero MR gradient artefacts). Nevertheless, the unprocessed gradient signals always provoke greater MSE values (the logarithmic ratio between MSE is never negative). The question as to why this difference can become so large (>37 dB in the case of zero MR gradients) arises. The difference between the ECG signal before and after filtering for both cases has therefore been investigated in more detail. It has been found that the unprocessed gradient signals (even if they are zero) introduced some small DC values into the filtered ECG signal (Fig. 3, Line 2). The adaptive filter with LMS coefficient updates requires zero-mean reference signals

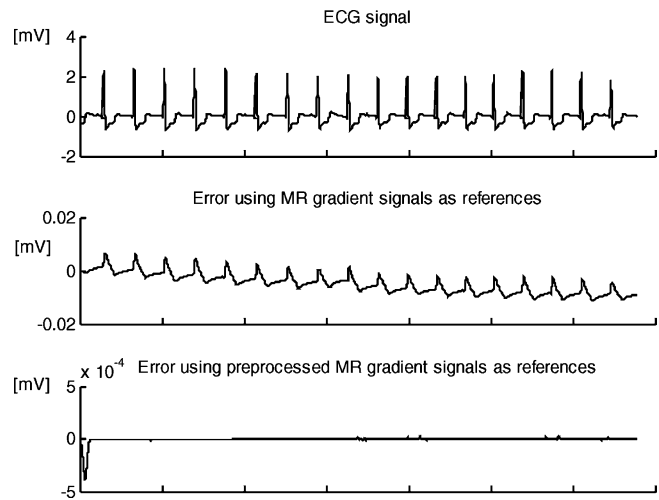


Fig. 3 The filter does not affect the ECG signal with zero MR gradient and when MR gradient artefacts do not occur (Line 1). The absolute value of the error signal (the difference between the unfiltered and filtered signals) is smaller than 1.1×10^{-2} when unprocessed gradient are used. It is smaller than 4.8×10^{-4} in the case of preprocessed gradients. The difference between the error signal for unprocessed gradients (Line 2) and preprocessed gradients (Line 3) is due a DC value which is provoked by the unprocessed gradients

[16], otherwise it can become unstable. Even the smallest DC noise component in the gradient signals (when gradient signals are zero, some weak noise will still be present) provokes such small DC components in the filtered ECG signal, the difference between unprocessed and preprocessed gradient signals may be an indicator of the stability of the filter (Table 1).

Good results have been found in the performance measurements with the ECG simulator. The reduction of the total average power of the noise was above 62% in all cases. The reduction of peak amplitudes is even greater ($>80\%$). This is due to a bias in the total average power caused by signal components that are not part of the MR gradient artefacts: firstly, the complete signal is used to estimate the total average power (even if no MR artefacts occurred during a signal segment), whereas only the MR gradient artefact segments of the acquired signal are used in the case of amplitude reduction. Therefore, any type of small noise (due to analogue–digital conversion, thermal noise, etc.) will be included in the calculation of the total average power. The value zero for the estimated total average power of the filtered signal is not possible for such signal segments. Furthermore, some small signal components of the ECG simulator signal are present in the estimated noise signal due to errors (the finite precision of the location of the R-wave) in the subtraction of the ECG from the acquired noisy signal (Fig. 4, Line 3). Secondly, the MR gradient artefact segments are not reduced equally. The reduction is highest for the peak amplitudes (see Fig. 4, Line 2 and Fig. 5) (Table 2).

Table 1 Calculation of the total average power of the ECG before filtering with (1) zero MR gradient signals and (2) undisturbed by MR gradient artefacts even if MR gradient signals are nonzero; logarithmic comparison between MSE of filtered and unfiltered ECG recordings using unprocessed and preprocessed gradient signals. For each subject, two different acquisitions were completed

Subjects	Total average power	Zero MR gradient signals		Nonzero MR gradient signals, but no artefacts found on ECG signal		
		Acquired ECG before filtering (μV^2)	MSE between ECG for zero MR gradient artefacts	MSE between ECG before/after filtering if the ECG signal did not include MR gradient artefacts	Logarithmic ratio between MSE	
		MSE ₁ : unprocessed gradient signals (μV^2)	MSE ₂ : preprocessed gradient signals (μV^2)	MSE ₁ : unprocessed gradient signals (μV^2)	MSE ₂ : preprocessed gradient signals (μV^2)	Logarithmic ratio between MSE
						$10 \times \log \left(\frac{MSE_1}{MSE_2} \right)$ (dB)
Volunteer 1	0.375	1.1×10^{-04}	1.4×10^{-13}	3.2×10^{-06}	1.4×10^{-06}	4
	0.383	7.9×10^{-06}	7.4×10^{-14}	1.5×10^{-06}	1.4×10^{-06}	0
Volunteer 2	1.540	8.0×10^{-04}	3.4×10^{-12}	8.8×10^{-03}	1.4×10^{-04}	18
	2.241	6.4×10^{-04}	3.6×10^{-10}	3.7×10^{-03}	5.1×10^{-05}	19
Patient 1	0.057	2.3×10^{-08}	1.4×10^{-13}	1.3×10^{-02}	2.7×10^{-04}	17
	0.129	1.9×10^{-05}	4.2×10^{-09}	1.3×10^{-02}	6.2×10^{-05}	23
Patient 2	0.207	6.2×10^{-08}	8.1×10^{-13}	9.2×10^{-04}	5.1×10^{-06}	23
	0.330	3.1×10^{-07}	4.1×10^{-12}	7.6×10^{-04}	7.2×10^{-06}	20
Patient 3	0.022	1.1×10^{-07}	2.2×10^{-14}	3.5×10^{-07}	3.4×10^{-07}	0
	0.017	1.2×10^{-07}	4.8×10^{-14}	1.4×10^{-07}	1.4×10^{-07}	0
Patient 4	0.419	2.6×10^{-07}	1.3×10^{-12}	1.4×10^{-02}	8.9×10^{-05}	22
	2.085	2.9×10^{-06}	1.5×10^{-12}	6.2×10^{-02}	9.2×10^{-04}	28

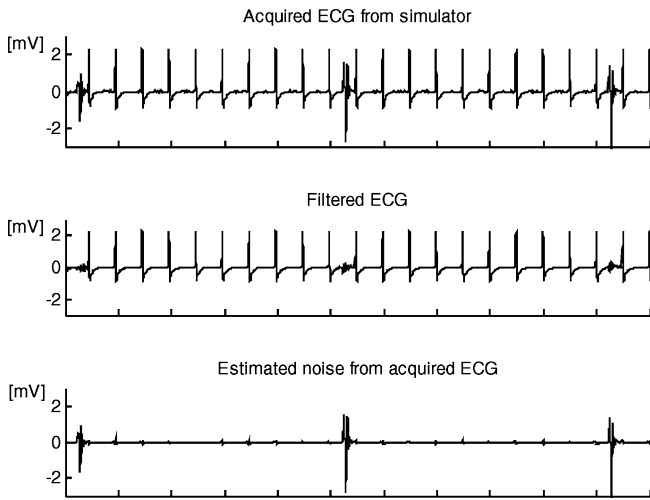


Fig. 4 The ECG simulator gave us the opportunity to extract the MR gradient noise (*line 3*) accurately and measure its total average power as well as the peak amplitudes for the performance tests of the adaptive filter

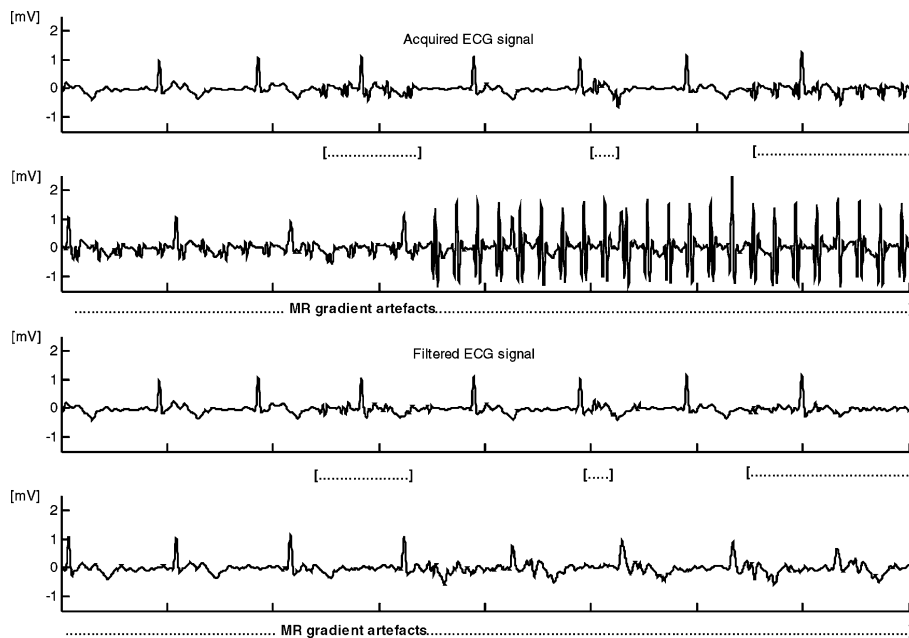


Fig. 5 The acquired ECG (*lines 1 and 2*) and the filtered ECG (*lines 3 and 4*) from a patient during a diffusion sequence (worst-case parameters: $B=1000$, $FOV=10$ cm, head image) is shown. The segments of the MR gradient artefacts of the signals have been marked by brackets for both cases. The reduction of the MR gradient artefacts is by 80% in the first segment and by more than 90% in the second part of the third segment. For small MR gradient artefacts (segments 1 and 2), the MR gradient artefacts partially remain. The MR gradient artefact suppression is more efficient for large amplitudes than for small ones, whereas some minor noise will always remain

It is best to use test 4 to mitigate errors caused by the subtraction of an estimated ECG (as in test 3 or 5). In

fact, the results for amplitude reduction are excellent for electrode placement on the arm or the leg as long as the total average power of the unfiltered MR gradient noise is greater than $0.010 \mu V^2$. In all other cases, the filtered noise is so small that it is covered by the other noise components and the calculation of the total average power of the filtered noise and the measurement of the amplitude reduction (could be rated as 100%) become impossible or may not be applicable for the performance measurement.

In the fifth test, the performance is calculated for signals that include MR gradient artefacts acquired from volunteers and patients. The total average power estimation of the MR gradient artefacts becomes impossible whenever worst-case scenarios have been used. The triggering of the acquired signal is impossible without prior knowledge. With prior ECG annotation, the signal-averaging techniques can be used to calculate the average ECG beat and subtract it from the noisy signal. This allows the estimation of the total average power. The total average power estimation of the acquired signal segments in which

no MR gradient artefacts occurred and the total average power estimation of the noisy signal (without subtraction of the ECG) has therefore been made. The results can be used as long as the total average power of the MR gradient noise is greater than the total average power of the ECG signal without MR gradient artefacts. If the total average power of the noisy signal becomes smaller than three times the total average power of the clear ECG, the measurement of the total average power reduction is biased (Patients 5, 6 and 7 in Table 4). The comparison of the MR gradient artefact amplitude peaks leads to a reduction of at least 80%. These results are comparable to the results of test 3.

Table 2 Calculation of total average power of simulator ECG signals before filtering, which is related to the heart rate; comparison between total average power and peak amplitudes of estimated MR gradient noise before and after filtering

ECG simulator heart rate (bpm)	Total average power			Reduction of total average power of noise (%)	Amplitude reduction of noise peaks (%)
	ECG (μV^2)	Estimated noise (μV^2)	Estimated filtered noise (μV^2)		
60	0.160	0.016	0.004	74	96–98
	0.161	0.015	0.004	75	99–100
65	0.186	0.030	0.010	66	85–89
	0.186	0.048	0.009	81	89–97
70	0.208	0.060	0.020	67	88–92
	0.210	0.060	0.023	62	80–99
80	0.260	0.107	0.032	71	85–97
	0.290	0.173	0.058	67	80–91
90	0.329	0.198	0.070	65	80–85
	0.391	0.280	0.074	74	80–93

Table 3 Comparison between total average power and peak amplitudes of signal acquired on volunteer's leg and arm, including MR gradient artefacts only. For each configuration, nine different acquisitions were done with a large range of total average power of the acquired MR gradient artefacts. The results in brackets are biased as the total average power of the filtered signal becomes so small that it is covered by other noise. In such cases, the calculation of the peak amplitude reduction has not been done (could be rated as 100%)

ECG recordings	Total average power		Comparison of total average powers (%)	Amplitude reduction of noise peaks (%)
	Unfiltered MR gradient artefacts (μV^2)	Filtered MR gradient artefacts (μV^2)		
Acquired on leg	0.004	<0.001	(82)	–
	0.006	<0.001	(85)	–
	0.018	<0.001	97	99
	0.025	<0.001	98	99
	0.026	<0.001	98	97–99
	0.034	<0.001	98	99
	0.036	0.002	94	96–99
	0.037	<0.001	98	99
	0.216	0.003	98	95–98
Acquired on arm	0.005	<0.001	(84)	–
	0.007	<0.001	(88)	–
	0.008	<0.001	(86)	–
	0.021	<0.001	97	99
	0.022	<0.001	97	99
	0.030	<0.001	98	98–99
	0.033	<0.001	98	99
	0.038	<0.001	98	97
	0.079	0.002	98	93–95

Discussion and conclusion

The adaptive filter with LMS coefficient updates can reduce gradient artefacts due to switching of the magnetic gradient field in real-time applications. The filter does not affect the desired ECG signal. Its computational efficiency allows easy implementation on a digital signal processor (DSP). The noise canceller can reduce nonlinear effects as

the MR gradient artefacts are reduced even if the reference signals are resampled to 500 Hz. The gradient signals are periodic and deterministic signals and their low- and high-frequency components have a strong time correlation. The adaptive filter therefore takes the low frequencies (which are in the same frequency band as the acquired ECG) of the gradient signal as reference for adaptation, even if the high frequency is the cause of the gradient artefacts. In this

Table 4 Calculation of total average power of ECG acquired on volunteers and patients before filtering; reduction of total average power of noisy signal and comparison of peak amplitudes of estimated MR gradient artefacts before and after filtering. For each subject, two different acquisitions were done. Results in brackets are biased as the total average power of the noisy signal is smaller than three times the total average power of the clear ECG

Subject	Total average power			Reduction of total average power of noisy ECG	Amplitude reduction of noise peaks (%)
	Clear ECG (μV^2)	Noisy ECG (μV^2)	Filtered ECG (μV^2)	$\frac{\text{Noisy ECG} - \text{filtered ECG}}{\text{filtered ECG}}$ (%)	
Volunteer 3	0.033	1.201	0.048	96	93–99
	0.047	0.207	0.044	79	88–99
Volunteer 4	0.010	0.261	0.021	92	98–99
	0.013	1.174	0.044	96	95–99
Volunteer 5	0.023	1.066	0.047	96	98–99
	0.024	0.059	0.022	63	84–87
Patient 5	1.900	1.982	1.903	(4)	85–97
	1.908	2.780	2.090	(25)	92–94
Patient 6	0.730	1.563	0.761	(51)	89–97
	0.741	2.123	0.750	65	83–86
Patient 7	0.157	0.189	0.158	(16)	80–82
	0.156	0.201	0.160	(20)	80–83

case, frequency folding or frequency modulation effects, which are nonlinear, will be taken into account by the adaptive filter as well as purely linear effects occurring in the frequency band of the acquired ECG. Furthermore, the adaptive filter does not require learning/adaptation when the amplitude in one gradient signal changes (i.e. phase gradient) while the others remain unchanged, as each gradient signal is taken as a single source of the gradient artefact generation effect and is associated with a separate transfer function. This is a major advantage over other methods which use a four-bit version of the current status of the MRI system [8] or a time-slice signal, as in [7].

The test methods 1 to 4 work well and in any case (even in worst-case scenarios). For test 5, prior knowledge about the trigger point and its annotation is required to estimate the total average power of the MR gradient artefacts correctly.

In conclusion, the reduction of the MR gradient artefact peaks was found to be 80–99%; the reduction of the total average power of the estimated noise was found to

be 62–98%. The quality of the corrected ECG is sufficient, that a standard one-lead QRS detector can be used for correct triggering/gating of the MR machine, for any type of MR imaging application. The ECG quality for permanent monitoring of the patient during an MR scan has not yet been achieved. Whenever the adaptive filter needs to (re)learn or considerably adapt one of the three transfer functions (due to changes such as: new sequence, major changes in the MR bore, major change of location of imaging slice, new patient, etc.), the gradient artefacts remain or are only partially removed.

Acknowledgements The study was supported by the Ministre de l'Industrie of France (RNTS 2003). The authors would like to thank the University Hospital Nancy, Brabois at Vandoeuvre-les-Nancy for the use of their MR machine and the support by the MR staff. Another thank you is addressed to the IADI laboratory staff. Furthermore, we thank SCHILLER Médical SAS, France, who supported us with all types of required hardware, and SCHILLER AG, Switzerland, for their financial and moral support.

References

1. Fischer SE, Wickline SA, Lorenz CH (1999) Novel real-time R-wave detection algorithm based on the vectorcardiogram for accurate gated magnetic resonance acquisitions. *Magn Reson Med* 42:361–370
2. Larson G, White RD, Laub G, McVeigh ER, Li D, Simonetti OP (2004) Self-gated cardiac. Cine MRI. *Magn Reson Med* 51:93–102
3. Keltner JR, Roos MS, Brakeman PR, Budinger TF (1990) Magnetohydrodynamics of blood flow. *Magn Reson Med* 16:139–149

4. Bonmassar G, Purdon PL, Jaaskelainen IP, Chiappa K, Solo V, Brown EN, Belliveau JW (2002) Motion and ballistocardiogram artifact removal for interleaved recording of EEG and EPs during MRI. *Neuroimage* 16:1127–1141
5. Felblinger J, Lehman C, Boesch C (1994) Electrocardiogram acquisition during MR examinations for patient monitoring and sequence triggering. *Magn Reson Med* 32:523–529
6. Lui F, Xia L, Crozier S (2003) Influence of magnetically-induced E-field on cardiac electric activity during MRI: a modelling study. *Magn Reson Med* 50:1180–1188
7. Allen PJ, Josephs O, Turner R (2000) A method for removing imaging artifact from continuous EEG recorded during functional MRI. *Neuroimage* 12:230–239
8. Sijbers J, Michiels I, Verhoye M, Van Audekerke J, Van der Linde A, Van Dyck D (1999) Restoration of MR-induced artifacts in simultaneously recorded MR/EEG data. *Magn Reson Med* 17:1383–1391
9. Goldman RI, Stern JM, Engel J, Coen MS (2000) Acquiring simultaneous ECG and functional MRI. *Clin Neurophysiol* 111:1974–1980
10. Felblinger J, Slotboom J, Kreis B, Jung B, Boesch C (1999) Restoration of electrophysiological signal distorted by inductive effects of magnetic field gradients during MRI sequences. *Magn Reson Med* 41:715–721
11. Kreger KS, Giordano CR (1992) Biopotential adaptive filtering in an MR environment abstracts SMRM 11th Annual scientific meeting 1:661
12. Yuan Q, Axel L, Hernandez EH, Dougherty L, Pilla JJ, Scott CH, Ferrari VA, Blom AS (2000) Cardiac-respiratory gating method for magnetic resonance imaging of the heart. *Magn Reson Med* 43:314–318
13. Shellock FG, Kanal E, (1996) Burns associated with the use of monitoring equipment during MR procedures. *J Magn Reson Imaging* 6:271–272
14. Kugel H, Bremer C, Püschel M, Fischbach R, Lenzen H, Tombach B, Van Aken H, Heindel W (2003) Hazardous situation in the MR bore: induction in ECG leads causes fire. *Eur Radiol* 13:690–694
15. Haykin S (1996) Adaptive filter theory. Prentice-Hall, New Jersey
16. Widrow B, Stearns SD (1985) Adaptive signal processing. Prentice-Hall, New Jersey